Semiclassical quantization of neutrino billiards

Barbara Dietz* and Zi-Yuan Li
School of Physical Science and Technology, and Key Laboratory for Magnetism and Magnetic Materials of MOE, Lanzhou University, Lanzhou, Gansu 730000, China

(Received 30 April 2020; accepted 30 September 2020; published 16 October 2020)

The impact of the classical dynamic on the fluctuation properties in the eigenvalue spectrum of nonrelativistic quantum billiards (QBs) are now well understood based on the semiclassical approach which provides an approximation for the fluctuating part $\rho^{\rm fluc}(k)$ of the spectral density in terms of a trace formula, that is, a sum over classical periodic orbits of its classical counterpart, abbreviated as CB. This connection between the eigenvalue spectrum of a quantum system and the classical periodic orbits is discernible in the Fourier transform of $\rho^{\rm fluc}(k)$ from eigenwave number k to length, which exhibits peaks at the lengths of the periodic orbits. The uprise of interest in properties of graphene related to their relativistic Dirac spectrum implicated the emergence of intensive studies of relativistic neutrino billiards (NBs), consisting of a spin-1/2 particle governed by the Dirac equation and confined to a bounded planar domain. In distinction to QBs, NBs do not have a well-defined classical limit. Yet comparison of their length spectra showed that for massless spin-1/2 particles those of the NB exhibit peaks at positions corresponding to the lengths of periodic orbits with an even number of reflections at the boundary of the CB associated with the corresponding QB. In order to understand the transition from the relativistic to the nonrelativistic regime, we derive an exact quantization condition for massive NBs and use it to obtain a trace formula. This trace formula provides a direct link between the spectral density of a NB and the classical dynamic of the corresponding QB through the periodic orbits of the associated CB.

DOI: 10.1103/PhysRevE.102.042214

I. INTRODUCTION

Billiards are particularly suited for theoretical, numerical, and experimental investigations within quantum chaos [1–3]. They consist of a bounded two-dimensional domain Ω, in which a point particle moves freely and is reflected specularly at the boundary $\partial\Omega$ and are referred to as classical billiards (CBs). Billiards have the nice feature that their dynamic is determined by their shape. The associated nonrelativistic quantum billiard (QB) is governed by the Schrödinger equation for a free particle which is confined to the billiard domain by imposing on the wave functions $\psi(\boldsymbol{r})$ the Dirichlet boundary condition (BC) $\psi(\boldsymbol{r}) = 0$ along the boundary $\boldsymbol{r} \in \partial\Omega$ [4–7]. Numerous numerical and also experimental studies have been performed [5,8–13] with billiards validating the Bohigas-Giannoni-Schmit conjecture [14–17] and the Berry-Tabor conjecture [18] concerning the universality of the spectral properties of quantum systems with fully chaotic and integrable classical counterpart, respectively, and their descriptiveness by random matrix theory for sufficiently large energies. Criteria for the applicability of random matrix theory could be finally identified within the periodic orbit (PO) theory employable to the semiclassical limit $\hbar \to 0$, which was pioneered by Gutzwiller [19,20]. It provides an approximation for the fluctuating part of the spectral density of a quantum system in terms of a sum over the POs of the associated classical dynamic, e.g., Gutzwiller's trace formula for chaotic systems [21].

Yet there also exist billiards with certain shapes which do not comply with these conjectures. Examples are billiards with a threefold-symmetric shape [22–24] or a unidirectional classical dynamic [25–28]. If the shape of such billiards has no further geometric symmetry, then the spectral properties coincide with those of generic chaotic systems with violated time-reversal invariance even though it is preserved. The deviations from the expected results could be explained in terms of semiclassical trace formulas [26,29–31]. In 1987 Berry and Mondragon proposed another example with these properties, neutrino billiards [32] (NBs). They are governed by the Dirac equation for a spin-1/2 particle which is confined to the billiard area by imposing the BC that there is no outward current. In Ref. [32] massless NBs, that is, massless spin-1/2 particles, were considered. It was shown in Ref. [32] that the associated Hamiltonian is not invariant under time reversal. Furthermore, the length spectra, i.e., the Fourier transform of the fluctuating part of the spectral density, exhibits peaks at the lengths of POs of the corresponding CB; however, in distinction to the corresponding QB, those with an odd number of reflections at the boundary are missing. These features were shown in Ref. [32] to have their origin in the chirality of such POs and they indicate that the spectral density of NBs can be written in terms of a trace formula over POs with an even number of reflections of the associated CB. Interest in NBs reemerged recently [33–44] with the pioneering fabrication of graphene [45–50] which entailed an increasing interest in the spectral properties of graphene billiards (GBs) [33,35,36,38,39,43,44,46,47], that is, finite-size sheets of (artificial) graphene.

*Dietz@lzu.edu.cn

In distinction to QBs, NBs do not have a well-defined classical limit. Therefore, the question arises whether their spectral properties are related to the classical dynamic of the CB of corresponding shape, as is the case for QBs. A direct link between a QB and its classical counterpart is provided by Gutzwiller's trace formula for systems with a chaotic classical dynamic and by a trace formula of Berry and Tabor for integrable systems [18]. The objective of the present article is to understand within such a semiclassical approach how the transition from a relativistic NB to a nonrelativistic QB of corresponding shape takes place. In Refs. [51,52] a semiclassical trace formula and semiclassical quantization rules were derived on the basis of Gutzwiller's method [4,19] for the Dirac equation of a charged relativistic particle with spin-1/2 exposed to an external static electromagnetic field. Furthermore, trace formulas were derived for GBs [39,53] subject to various BCs using a multiple reflection expansion. In Ref. [54] a trace formula was obtained for massless circular and elliptical NBs, i.e., for the ultrarelativistic case, following the procedure of Refs. [55–57] for QBs which uses a boundary-integral equation (BIE) as starting point, yielding a secular equation in terms of a spectral determinant [58–60]. We derive a trace formula for massive NBs which also makes use of the results of Refs. [55–57]. For this we derive an exact BIE of which the solutions yield the eigenstates of massive NBs. They render possible the derivation of a semiclassical quantization condition for NBs which then is used to obtain the trace formula. In Ref. [61] the features of quantum scars and spectral properties of massive NBs were investigated. The eigenvalues were obtained with a numerical procedure yielding eigenstates which do not fully comply with the BC for NBs. The BIE has the advantage that it originates from the Green's theorem and, therefore, incorporates the BC, which is crucial for the derivation of the trace formula.

In Sec. II we briefly review the Dirac equation for NBs, that is, of a spin-1/2 particle of mass m confined to the billiard domain by imposing a BC on the spinor wave function which links its components. In order to enable the analytical study of the transition from relativistic NBs to nonrelativistic QBs we turn this BC into BCs imposed on each spinor wave-function component separately. Then we introduce in Sec. III the BIEs for massive neutrino billiards. In Sec. IV we consider the nonrelativistic limit, where the energy is close to the rest energy, $E \simeq mc^2$, which is reached in the limit $\beta = \frac{mc}{\hbar k} \to \infty$ for fixed, nonzero $\hbar k$ with k denoting the free-space wave vector, i.e., for $mc \to \infty$. We verify that the nonrelativistic limit complies with the BCs for massive NBs yielding that the spinor components decouple in that limit and their wave equations coincide with those of QBs subject to Robin boundary conditions. In Sec. V we derive the trace formula attained for a given value of mc in the semiclassical limit $\hbar \to 0$ while keeping $\hbar k$, that is, β fixed, using similar methods as in Ref. [54]. A fundamental problem of trace formulas in general is their convergence. They can, for example, arise due to POs which move nearly tangential to the boundary [62,63]. We will address the convergence problem and test it for the trace formula of a massive circle NB, which we derive in Sec. VI. In Sec. VII we compare our results to those for a constant-width NB. Using the fact that NBs and QBs are scale invariant, we fix the range of β by choosing for all realizations the same range of k values, where the minimum value is set equal to that of the smallest eigenvalue taken into account, and consider neutrino billiards of increasing mass. That is, we increase $\tilde{\beta}$ until the trace formula coincides with that of the corresponding QB. For both NBs we come to the result that the nonrelativistic limit is reached for a finite value of β.

II. THE DIRAC EQUATION FOR NBS

The Dirac equation of a free spin-1/2 particle of mass m moving with momentum $\hat{\boldsymbol{p}} = -i\hbar\nabla$ in the $\boldsymbol{r} = (x, y)$ plane reads

$$c\hat{\boldsymbol{\sigma}} \cdot \hat{\boldsymbol{p}}\boldsymbol{\psi} = [E\,\mathbb{1} - mc^2\hat{\boldsymbol{\sigma}}_z]\boldsymbol{\psi},\ \boldsymbol{\psi} = \begin{pmatrix}\psi_1\\ \psi_2\end{pmatrix}. \tag{1}$$

Here $\mathbb{1}$ is the 2×2 unit matrix, $\hat{\boldsymbol{\sigma}} = (\hat{\boldsymbol{\sigma}}_x, \hat{\boldsymbol{\sigma}}_y)$ and $\hat{\boldsymbol{\sigma}}_q$, $q = x, y, z$ denote the Pauli matrices. Furthermore, $E = \hbar c k_E = \hbar ck\sqrt{1+\beta^2}$ is the energy of the particle where k is the free-space wave vector and $\beta = \frac{mc}{\hbar k}$ denotes the ratio of the rest-energy momentum and free-space momentum.

We are interested in the properties of the eigenstates of massive NBs with a smooth boundary and no diffractive corners. For massless spin-1/2 particles confinement of the particle to the billiard domain Ω is achieved [32] by requiring that the Hamiltonian of a closed system should preserve self-adjointness, implying that it is Hermitian. This property is not destroyed when introducing the mass term in Eq. (1). Accordingly, the BCs are independent of the size of m. Defining the boundary $\partial\Omega$ of the NB by $\boldsymbol{r}(s) = [x(s), y(s)]$ in coordinate space or by $w(s) = x(s) + iy(s)$ in the complex plane through the arc-length parameter $s \in [0, \mathcal{L}]$ with $\mathcal{L}$ denoting the perimeter, the BC reads

$$\psi_2(s) = ie^{i\alpha(s)}\psi_1(s). \tag{2}$$

Here $\alpha(s)$ is the angle of the outward-pointing normal vector $\mathbf{n}(s) = [\cos\alpha(s), \sin\alpha(s)]$ with respect to the x axis at $\boldsymbol{r}(s)$. The BC links the wave-function components $\psi_{1,2}(s)$ at $\partial\Omega$. For the derivation of separate BCs we introduce local coordinates (n, s) along the boundary ($n = 0$, s) in the directions of $\boldsymbol{n}(s)$ and of the tangential vector $\boldsymbol{t}(s) = [-\sin\alpha(s), \cos\alpha(s)]$ to $\partial\Omega$ at $\boldsymbol{r}(s)$. Denoting the normal and tangential derivatives along $\partial\Omega$ by $\partial_n = \boldsymbol{n}\cdot\nabla$ and $\partial_s = \boldsymbol{t}\cdot\nabla$, respectively, yielding $\partial_x \pm i\partial_y = e^{\pm i\alpha(s)}(\partial_n \pm i\partial_s)$ and applying Eq. (2), we obtain from Eq. (1) for the BCs of the wave-function components along $\partial\Omega$

$$\begin{aligned}(\partial_n + i\partial_s)\psi_1(n,s)|_{n\to0^-} &= -k\mathcal{K}^{-1}\psi_1(s),\\ (\partial_n - i\partial_s)\psi_2(n,s)|_{n\to0^-} &= k\mathcal{K}\psi_2(s),\end{aligned} \tag{3}$$

where $n \to 0^-$ means that the boundary is approached in direction of $\boldsymbol{n}(s)$ from the interior. Note that we suppress in the boundary wave functions the first argument of $\psi_{1,2}(n = 0, s) = \psi_{1,2}(s)$. Furthermore, we introduced

$$\mathcal{K} = \sqrt{\frac{\sqrt{1+\beta^2}-\beta}{\sqrt{1+\beta^2}+\beta}} = \sqrt{\frac{1-\sin\theta_\beta}{1+\sin\theta_\beta}}, \tag{4}$$

$$\cos\theta_\beta = \frac{1}{\sqrt{1+\beta^2}},\quad \sin\theta_\beta = \frac{\beta}{\sqrt{1+\beta^2}}. \tag{5}$$

For massless particles $\mathcal{K}=1$ and $\theta_\beta=0$, whereas in the nonrelativistic limit $\beta\to\infty$ [64] $\mathcal{K}\simeq\frac{1}{2\beta}\to 0$, and $\theta_\beta\to\pi/2$. We use the variable θ_β instead of β in order to facilitate a well-defined nonrelativistic limit as outlined in following sections. Introducing in the vicinity of the boundary the wave functions

$$\Phi_1(n,s)=\{\psi_1(n,s)+[-ie^{-i\alpha(s)}]\psi_2(n,s)\}/2,$$
$$\Phi_2(n,s)=\{\psi_2(n,s)+[ie^{i\alpha(s)}]\psi_1(n,s)\}/2, \tag{6}$$

with $\Phi_{1,2}(n,s)\xrightarrow{n\to 0^-}\psi_{1,2}(s)$, that are used below for the evaluation of the BIEs, the BCs [Eq. (3)] become

$$\left[\tilde\beta+\tfrac{1}{2}\kappa(s)\right]\Phi_j(s)+\partial_n\Phi_j(n,s)|_{n\to 0^-}=0,\quad j=1,2, \tag{7}$$

with $\tilde\beta=\frac{mc}{\hbar}$ corresponding to the rest-energy momentum in units of $\hbar$ and $\kappa(s)=\frac{d}{ds}\alpha(s)$ denoting the curvature of the boundary at $\boldsymbol{r}(s)$. Here we use the BC Eq. (2) which implies that

$$i\partial_s\psi_2(s)=-\kappa(s)\psi_1(s)+ie^{i\alpha(s)}i\partial_s\psi_1(s). \tag{8}$$

According to Eq. (7) $\Phi_{1,2}(s)$ obey Robin BCs [65–67]; however, they are linked by Eq. (2).

III. BOUNDARY-INTEGRAL EQUATIONS FOR MASSIVE NBS

In order to derive a BIE for massive neutrino billiards, we divide $\psi_{1,2}(\boldsymbol{r})$ in Eq. (1) by the amplitudes of the corresponding free-space wave-function components [64], that is, introduce the two-component spinor $\tilde{\boldsymbol{\psi}}(\boldsymbol{r})$ through

$$\boldsymbol{\psi}=\begin{pmatrix}\sqrt{\frac{E+mc^2}{2E}}\tilde\psi_1\\ \sqrt{\frac{E-mc^2}{2E}}\tilde\psi_2\end{pmatrix}=\begin{pmatrix}\sqrt{\frac{1+\sin\theta_\beta}{2}}\tilde\psi_1\\ \sqrt{\frac{1-\sin\theta_\beta}{2}}\tilde\psi_2\end{pmatrix}, \tag{9}$$

yielding for the Dirac equation of a massive NB

$$k\tilde{\boldsymbol{\psi}}(\boldsymbol{r})+i\hat{\boldsymbol{\sigma}}\cdot\nabla\tilde{\boldsymbol{\psi}}(\boldsymbol{r})=0, \tag{10}$$

$$\tilde\psi_2(s)=ie^{i\alpha(s)}\mathcal{K}^{-1}\tilde\psi_1(s). \tag{11}$$

For $\beta\to 0$ Eq. (10) together with the BC Eq. (11) approaches the Dirac equation for a massless NB.

The Dirac equation (10) has the same form as that for a massless spin-1/2 particle, except for modified BCs. Accordingly, we may proceed as in Refs. [32,67] to derive BIEs for the wave-function components and then as in Ref. [54] to obtain a semiclassical approximation for the fluctuating part $\rho^{\rm fluc}(k;\tilde\beta)$ of the spectral density. After applying the BC Eq. (10) the BIEs become

$$\tilde\psi_1^*(s')=\frac{ik}{2}\oint_{\partial\Omega}ds\tilde\psi_1^*(s)\big\{-\mathcal{K}^{-1}H_0^{(1)}[k\rho(s,s')]+e^{-i\alpha(s)}e^{i\xi(s,s')}H_1^{(1)}[k\rho(s,s')]\big\}, \tag{12}$$

$$\tilde\psi_2^*(s')=\frac{ik}{2}\oint_{\partial\Omega}ds\tilde\psi_2^*(s)\times\big\{\mathcal{K}H_0^{(1)}[k\rho(s,s')]+e^{i\alpha(s)}e^{-i\xi(s,s')}H_1^{(1)}[k\rho(s,s')]\big\}, \tag{13}$$

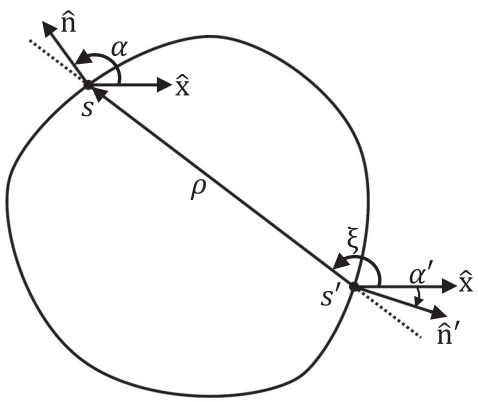

FIG. 1. Illustration of the quantities entering Eqs. (12) and (13). Here $\hat{\boldsymbol{x}}$ denotes the x axis. The billiard has the shape of the constant-width NB considered in Sec. VII.

with (see Fig. 1)

$$e^{i\xi(s,s')}=\frac{\boldsymbol{r}(s)-\boldsymbol{r}(s')}{|\boldsymbol{r}(s)-\boldsymbol{r}(s')|},\quad \rho(s,s')=|\boldsymbol{r}(s)-\boldsymbol{r}(s')|. \tag{14}$$

Here $H_m^{(1)}(k\rho)=J_m(k\rho)+iY_m(k\rho)$ refers to the Hankel function of the first kind of order m. We show in Sec. A of the Appendix that these BIEs yield the analytically known eigenstates of a massive circle NB. In Sec. B of the Appendix we outline how it can be shown that these equations indeed fulfill the boundary conditions Eq. (3) and thus Eq. (7).

We note that, independently of the value of β, the BIEs (12) and (13) can be brought to the form of the BIE for QBs by applying the BCs Eq. (3) and using that

$$\oint_{\partial\Omega}dsH_0[k\rho(s,s')]\partial_s\tilde\psi_j^*(s)=-\oint_{\partial\Omega}ds\tilde\psi_j^*(s)\partial_sH_0[k\rho(s,s')]$$

and

$$\partial_sH_0^{(1)}[k\rho(s,s')]=-k\sin(\xi-\alpha)H_1^{(1)}[k\rho(s,s')], \tag{15}$$

yielding

$$\frac{1}{2}\tilde\psi_j^*(s')=\oint_{\partial\Omega}ds\{\tilde\psi_j^*(s)\partial_nG_0[s',s;k]-G_0[s',s;k]\partial_n\tilde\psi_j^*(s)\}, \tag{16}$$

for $j=1,2$. Here

$$G_0[s',s;k]=-\frac{i}{4}H_0^{(1)}[k\rho(s,s')] \tag{17}$$

is the free-space Green's function in the plane. This is the BIE for the nonrelativistic Schrödinger equation [68] of a QB of corresponding shape. Actually, applying $-i\hbar\hat{\boldsymbol{\sigma}}\cdot\boldsymbol{\nabla}$ to the Dirac equation (1) yields for both wave-function components the Schrödinger equation of a free particle. However, they are linked through the BC Eq. (2).

At $\rho=0$ $H_0(k\rho)$ and $H_1(k\rho)$ have a logarithmic and $1/\rho$ singularity, respectively. The latter is removed by switching from the wave-function components $\psi_{1,2}^*$ to their combinations $\Phi_{1,2}^*$ given in Eq. (6) and using the BC Eq. (2), leading

to the BIE

$$\begin{aligned}\cos\theta_\beta\tilde{\psi}_1^*(s') &= \frac{ik}{4}\oint_{\partial\Omega} ds 2e^{i\frac{\Delta\Phi(s,s')}{2}}\tilde{\psi}_1^*(s)\\ &\times\left(\left\{i\sin\left[\frac{\Delta\Phi(s,s')}{2}\right]-\sin\theta_\beta\cos\left[\frac{\Delta\Phi(s,s')}{2}\right]\right\}\right.\\ &\times H_0^{(1)}(k\rho)\\ &\left.+\cos\theta_\beta\cos\left[\frac{\alpha(s')+\alpha(s)}{2}-\xi(s,s')\right]H_1^{(1)}(k\rho)\right), \quad (18)\end{aligned}$$

where $\Delta\Phi(s,s')=\frac{\alpha(s')-\alpha(s)}{2}$. Furthermore, in the remainder of the paper we suppress the argument of $\rho=\rho(s,s')$. The corresponding equation for $\tilde{\psi}_2^*(s')$ is obtained with Eq. (11) by multiplying the integrand with $e^{-i\Delta\Phi(s,s')}$. The ultrarelativistic and nonrelativistic cases are attained for $\theta_\beta=0$ and $\theta_\beta=\frac{\pi}{2}$, respectively. For $s\to s'$, i.e., $\rho\to 0$ all terms in the integrand vanish [67] except for the one proportional to $\sin\theta_\beta H_0^{(1)}(k\rho)$, which vanishes for massless particles and otherwise contains a logarithmic singularity that can be dealt with for billiards with a smooth boundary and no diffractive corners [69]. This singularity can be removed by using relation Eq. (B1) obtained by imposing on $\tilde{\psi}_1(s')$ and $\tilde{\psi}_2(s')$ the BC Eq. (11) using the right-hand sides of Eqs. (12) and (13). Then the BIE Eq. (18) becomes

$$\begin{aligned}\tilde{\psi}_1^*(s') &= \frac{ik}{4}\oint_{\partial\Omega} ds e^{i\frac{\Delta\Phi(s,s')}{2}}2\tilde{\psi}_1^*(s)\\ &\times\left\{i\cos\theta_\beta\sin\left[\frac{\Delta\Phi(s,s')}{2}\right]H_0^{(1)}(k\rho)\right.\\ &+i\sin\theta_\beta\sin\left[\frac{\alpha(s')+\alpha(s)}{2}-\xi(s,s')\right]H_1^{(1)}(k\rho)\\ &\left.+\cos\left[\frac{\alpha(s')+\alpha(s)}{2}-\xi(s,s')\right]H_1^{(1)}(k\rho)\right\}. \quad (19)\end{aligned}$$

For $s\to s'$ the first and the last terms vanish [67], whereas the second term approaches

$$\begin{aligned}&2ie^{i\frac{\Delta\Phi(s,s')}{2}}\sin\theta_\beta\sin\left[\frac{\alpha(s')+\alpha(s)}{2}-\xi(s,s')\right]\frac{ik}{4}H_1^{(1)}(k\rho)\\ &\xrightarrow{s\to s'}\frac{\sin\theta_\beta}{2\pi}\left[-\kappa(s)+i\frac{d}{ds}\frac{1}{r'(s)}\right], \quad (20)\end{aligned}$$

where $r'(s)=\frac{d}{ds}|\boldsymbol{r}|$. Equation (19) is of particular usefulness for the high-precision computation of the eigenvalues of massive NBs.

The correponding BIEs for the wave-function components $\psi_{1,2}$ are obtained by multiplying them with the prefactors defined in Eq. (9) that relate them to $\tilde{\psi}_{1,2}$, that is, their BIEs are given by Eqs. (12) and (13) with $\tilde{\psi}_{1,2}$ replaced by $\psi_{1,2}$.

IV. THE NONRELATIVISTIC LIMIT

The nonrelativistic limit is attained by increasing β at a fixed, nonzero value of $\hbar k$ until the energy is close to the rest energy, and it is reached when $E\simeq mc^2+(\hbar k)^2/(2m)$. Then, the equation for the second wave-function component in (1) becomes

$$\psi_2(\boldsymbol{r})\simeq-\frac{i}{2\tilde{\beta}}(\partial_x+i\partial_y)\psi_1(\boldsymbol{r}), \quad (21)$$

yielding for the first one when inserting this relation

$$\left(-\frac{\hbar^2}{2m}\Delta+k^2\right)\psi_1(\boldsymbol{r})=0. \quad (22)$$

To check whether this functional dependence of $\psi_2(\boldsymbol{r})$ on $\psi_1(\boldsymbol{r})$ complies with the BCs Eq. (3), we consider Eq. (21) along the boundary $\partial\Omega$,

$$\begin{aligned}\psi_2(s) &= -\frac{i}{2\tilde{\beta}}e^{i\alpha(s)}(\partial_n+i\partial_s)\psi_1(n,s)|_{n\to 0^-}, \quad (23)\\ &\overset{!}{=}\frac{i}{2\beta}e^{i\alpha(s)}\mathcal{K}^{-1}\psi_1(s), \quad (24)\\ &=\frac{\mathcal{K}^{-1}}{2\beta}\psi_2(s), \quad (25)\end{aligned}$$

where we used Eqs. (2) and (3) for the second and third equalities, respectively. This implies that $\mathcal{K}^{-1}\simeq 2\beta$ must hold, which is the case for sufficiently large β. Then $\psi_1(\boldsymbol{r})$ decouples from $\psi_2(\boldsymbol{r})$ and the boundary wave functions $\Phi_j(s)$ coincide with the wave-function components, $\Phi_j(n,s)\equiv\psi_j(n,s)$. Accordingly, $\psi_1(\boldsymbol{r})$ may be determined by solving the Schrödinger equation of a QB subject to the Robin BC [Eq. (7)], which turns into the Dirichlet BC for $\tilde{\beta}\to\infty$ [43,70]. A trace formula, that is, a semiclassical approximation, has been derived for the spectral density of such QBs [65].

V. A SEMICLASSICAL QUANTIZATION RULE FOR NBS

In the rest of the paper we will consider the semiclassical limit $\hbar\to 0$ for fixed $E=\hbar ck_E$ and $\hbar k$, i.e., for fixed β and thus mc, which is equivalent to taking the limit of k_E or of k to ∞ while leaving β and mc unchanged. In the derivation we assume that the NB has the shape of a CB with chaotic classical dynamics. To obtain a semiclassical quantization condition which is well defined for all values $0\leqslant m<\infty$, i.e., $0\leqslant\theta_\beta\leqslant\pi/2$, and yields a trace formula with convergence properties similar to those of Gutzwiller's trace formula, we use as starting point a combination of Eq. (18) and a BIE resulting from the BC [Eq. (7)],

$$\begin{aligned}\left[\sin\theta_\beta+\frac{\kappa(s')}{2k}\right]\tilde{\psi}_1^*(s') &= \frac{ik}{4}\oint_{\partial\Omega} ds 2e^{i\frac{\Delta\Phi(s,s')}{2}}\tilde{\psi}_1^*(s)\cos\left[\xi(s,s')-\alpha(s')\right] \quad (26)\\ &\times\left(\cos\theta_\beta\cos\left[\frac{\alpha(s')+\alpha(s)}{2}-\xi(s,s')\right]H_0^{(1)}(k\rho)\right.\end{aligned}$$

$$-\left\{i\sin\left[\frac{\Delta\Phi(s,s')}{2}\right]-\sin\theta_\beta\cos\left[\frac{\Delta\Phi(s,s')}{2}\right]\right\}H_1^{(1)}(k\rho)\Big)$$
$$-\cos\theta_\beta\frac{ik}{4}\oint_{\partial\Omega}ds\tilde{\psi}_1^*(s)\left\{e^{i[2\xi(s,s')-\alpha(s')-\alpha(s)]}+e^{2i[\alpha(s')-\xi(s,s')]}\right\}\frac{H_1^{(1)}(k\rho)}{k\rho}. \quad (27)$$

More details are provided in Sec. B of the Appendix. Again, the corresponding equation for $\tilde{\psi}_2^*(s')$ is obtained with Eq. (11) by multiplying the integrand with $e^{-i\Delta\Phi(s,s')}$. For billiard shapes with no diffractive corners $\frac{\kappa(s)}{k}$ and also the term (27) become negligible in the semiclassical limit $k\to\infty$. Note that the left-hand side of Eq. (18) vanishes in the nonrelativistic limit $\theta_\beta=\pi/2$, whereas that of Eq. (26) is zero in the ultrarelativistic limit $\theta_\beta=0$. However, the derivation of a trace formula based on a BIE requires that it is nonvanishing. Since both BIEs apply in the semiclassical limit, we may use the sum of Eq. (18) multiplied with $\cos\theta_\beta$ and Eq. (26) multiplied with $\sin\theta_\beta$ to overcome this problem. The resulting quantization condition can be cast to the form [54,56]

$$\tilde{\boldsymbol{\psi}}^\dagger[\boldsymbol{r}(s')]=\oint_{\partial\Omega}dsQ[\boldsymbol{r}(s'),\boldsymbol{r}(s);k]\tilde{\boldsymbol{\psi}}^\dagger[\boldsymbol{r}(s)]$$
$$=\hat{\boldsymbol{Q}}(k)\tilde{\boldsymbol{\psi}}^\dagger[\boldsymbol{r}(s)], \quad (28)$$

with $\hat{\boldsymbol{Q}}_{ij}(k)=\hat{\boldsymbol{Q}}_{jj}(k)\delta_{ij}$ denoting the integral operator which is applied to $\tilde{\psi}_j^*(s)$ to obtain $\tilde{\psi}_j^*(s')$. This equation has nontrivial solutions at the zeros of the spectral determinant, leading to the quantization condition

$$\det[\mathbb{1}-\hat{\boldsymbol{Q}}(k)]=0. \quad (29)$$

Thus, the fluctuating part of the spectral density is related to the trace of $\hat{\boldsymbol{Q}}^p(k)$ through [56,57]

$$\rho^{\rm fluc}(k;\tilde{\beta})=-\frac{1}{\pi}{\rm Im}\frac{d}{dk}\ln\det[\mathbb{1}-\hat{\boldsymbol{Q}}(k)], \quad (30)$$
$$=\frac{1}{\pi}{\rm Im}\sum_{p=1}^{\infty}\frac{1}{p}\frac{d}{dk}[{\rm Tr}\hat{\boldsymbol{Q}}^p(k)], \quad (31)$$

where

$${\rm Tr}\hat{\boldsymbol{Q}}^p(k)=\oint_{\partial\Omega}ds_1\oint_{\partial\Omega}ds_2\cdots\oint_{\partial\Omega}ds_p\mathcal{P}_p. \quad (32)$$

Here

$$\mathcal{P}_p=2\cos\left[\sum_{r=1}^{p}\frac{\Delta\Phi(s_{r+1},s_r)}{2}\right]\prod_{r=1}^{p}Q[\boldsymbol{r}(s_r),\boldsymbol{r}(s_{r+1});k] \quad (33)$$

with $s_{p+1}=s_1$, $s_0=s_p$, and $Q[\boldsymbol{r}(s_r),\boldsymbol{r}(s_{r+1});k]$ can be read off the terms in round brackets in Eq. (18) multiplied with $\cos\theta_\beta$ and in Eq. (26) multiplied with $\sin\theta_\beta$. To solve the p integrals we use the results obtained for the corresponding QB in the semiclassical limit (see the Appendix of Ref. [56]). For this we extract from $Q[\boldsymbol{r}(s_r),\boldsymbol{r}(s_{r+1});k]$, that is, from Eqs. (18) and (26) the Hankel functions, where we use the relation Eq. (17) and the following approximations valid for $k\to\infty$,

$$G_0[\boldsymbol{r}(s),\boldsymbol{r}(s');k]\simeq-\frac{i}{4}\sqrt{\frac{2}{\pi\rho}}e^{ik\rho-\frac{i}{4}\pi}, \quad (34)$$
$$H_1(k\rho)\simeq\frac{1}{i}H_0(k\rho), \quad (35)$$

and

$$\partial_{n'}G_0[\boldsymbol{r}(s),\boldsymbol{r}(s');k]$$
$$\simeq i\cos[\alpha(s')-\xi(s,s')]\cdot(-k)\cdot G_0[\boldsymbol{r}(s),\boldsymbol{r}(s');k], \quad (36)$$

to cast Eq. (32) to the form

$${\rm Tr}\hat{\boldsymbol{Q}}^p(k)$$
$$\simeq(-2)^p\times\oint_{\partial\Omega}ds_1\cdots\oint_{\partial\Omega}ds_p\prod_{r=1}^{p}\partial_{n_r}G_0[\boldsymbol{r}(s_r),\boldsymbol{r}(s_{r+1});k]$$
$$\times\left(\frac{i}{2}\right)^p\frac{\tilde{\mathcal{P}}_p}{\prod_{r=1}^{p}\cos[\alpha_r-\xi_{r+1,r}]}. \quad (37)$$

We used the short cuts $\alpha_r=\alpha(s_r)$ and $\xi_{r+1,r}=\xi(s_{r+1},s_r)$ which denote the angles of the outward-pointing normal vector at s_r and of the trajectory segment connecting the reflection points at s_r and s_{r+1} with respect to the x axis, respectively. The difference between this term and that evaluated in Ref. [56] is that it has an additional factor given in the last line. Here $\tilde{\mathcal{P}}_p$ results from Eq. (33) after extraction of the Hankel functions [54]. The p integrals were performed in Ref. [56] by replacing the Green's functions by their asymptotic expressions Eq. (34) and applying the stationary phase approximation. Since the additional factor does not oscillate rapidly with k, it does not contribute to the stationary phase and we can adopt these results. In the semiclassical limit, the nonvanishing contributions to ${\rm Tr}\hat{\boldsymbol{Q}}^p(k)$ thus come from the POs of order p. Furthermore, the leading-k contribution to the derivative with respect to k in Eq. (32) comes from the phase factor resulting from the integrals over the normal derivatives of G_0. Accordingly, to leading order in k the saddle point approximation yields

$${\rm Im}\frac{1}{p}\frac{d}{dk}[{\rm Tr}\hat{\boldsymbol{Q}}^p(k)]$$
$$\simeq{\rm Re}\sum_{\gamma_p}\mathcal{A}_{\gamma_p}e^{i\Theta_{\gamma_p}}\frac{\tilde{\mathcal{P}}_p^*}{\prod_{r=1}^{p}(-2i)\cos[\alpha_r-\xi_{r+1,r}]}, \quad (38)$$

with

$$\mathcal{A}_{\gamma_p}=\frac{l_{\rm PO}^{(p)}}{r_{\rm PO}\sqrt{|{\rm Tr}M_{\rm PO}^{(p)}-2|}},\quad \Theta_{\gamma_p}=kl_{\rm PO}^{(p)}-\frac{\pi}{2}\mu_{\rm PO}^{(p)}. \quad (39)$$

The * in $\tilde{\mathcal{P}}_p^*$ indicates that the product should be evaluated along the POs. These are subject to the condition for specular reflection [32],

$$\xi_{r+1,r}-\alpha_r=\alpha_r-\xi_{r,r-1}+\pi. \quad (40)$$

Furthermore, $M_{\rm PO}^{(p)}$ denotes the monodromy matrix, $l_{\rm PO}^{(p)}$ the length of the PO, $\mu_{\rm PO}^{(p)}$ the Maslov index, and $r_{\rm PO}$ the number of

repetitions of the primitive PO. Gutzwiller's trace formula for QBs is attained when the last factor in Eq. (38) equals unity,

$$\rho_{\mathrm{QB}}^{\mathrm{fluc}}(k)=\frac{1}{\pi}\sum_{p=1}^{\infty}\sum_{\gamma_p}\mathcal{A}_{\gamma_p}\cos(\Theta_{\gamma_p}). \tag{41}$$

Note that it was shown in Ref. [54] that a trace formula is obtained for massless NBs, i.e., for $\theta_\beta=0$ in Eq. (38), with circular and elliptic shapes, which generate a regular classical dynamics, by replacing the amplitude $\mathcal{A}_{\gamma_p}$ and phase Θ_{γ_p} in Eq. (39) by those of the trace formula of the corresponding QB. We will demonstrate in Sec. VI that thereby a trace formula is also obtained for massive circular NBs. Introducing the angle

$$\chi_r=\xi_{r,r-1}-\alpha_r=\pi-(\xi_{r+1,r}-\alpha_r),\quad 0\leqslant\chi_r<\pi/2, \tag{42}$$

which yields $\xi_{r,r-1}$ with respect to the normal vector at s_r, the product $\tilde{\mathcal{P}}_p^*$ reads

$$\begin{aligned}\tilde{\mathcal{P}}_p^*=&\left(\frac{2}{i}\right)^p 2\cos\left(\Phi_{\gamma_p}-p\frac{\pi}{2}\right)\\&\times\prod_{r=1}^{p}\{\cos\theta_\beta+i\sin\theta_\beta\cos(\alpha_r-\xi_{r+1,r})\}\\&\times\left[\cos\left(\frac{\chi_r+\chi_{r+1}}{2}\right)-i\sin\theta_\beta\sin\left(\frac{\chi_r+\chi_{r+1}}{2}\right)\right.\\&\left.+\cos\theta_\beta\sin\left(\frac{\chi_r-\chi_{r+1}}{2}\right)\right].\end{aligned} \tag{43}$$

Here we used the following relations deduced from Eq. (40):

$$\frac{\alpha_{r+1}+\alpha_r}{2}-\xi_{r+1,r}=(\chi_r-\chi_{r+1})/2-\pi/2, \tag{44}$$

$$\alpha_{r+1}-\alpha_r=\pi-(\chi_r+\chi_{r+1}), \tag{45}$$

and

$$\Phi_{\gamma_p}=\sum_{r=1}^{p}\chi_r. \tag{46}$$

Using the rule of specular reflection Eq. (40) Φ_{γ_p} can be further evaluated,

$$\begin{aligned}\Phi_{\gamma_p}-p\frac{\pi}{2}&=\sum_{j=1}^{p}[\xi_{j,j-1}-\alpha_j]-p\frac{\pi}{2}\\&\equiv\sum_{j=1}^{p}\frac{[\xi_{j,j-1}-\xi_{j+1,j}]}{2}\\&=\frac{\xi_{1,0}-\xi_{p+1,p}}{2}.\end{aligned} \tag{47}$$

Here $\xi_{p+1,p}-\xi_{1,0}=N_p 2\pi$ is the complete phase accumulated after looping the PO, which is an integer multiple of 2π [32] denoted as N_p,

$$\Phi_{\gamma_p}-p\frac{\pi}{2}=-N_p\pi. \tag{48}$$

Equation (38) is brought to the form

$$\mathrm{Im}\frac{1}{p}\frac{d}{dk}[\mathrm{Tr}\hat{\boldsymbol{Q}}^p(k)], \tag{49}$$

$$=\mathrm{Re}\sum_{\gamma_p}2\cos\left(\Phi_{\gamma_p}-p\frac{\pi}{2}\right)\mathcal{B}_{\gamma_p}^{\tilde{\beta}}e^{i\Gamma_{\gamma_p}^{\tilde{\beta}}}\mathcal{A}_{\gamma_p}e^{i\Theta_{\gamma_p}}, \tag{50}$$

where $\mathcal{B}_{\gamma_p}^{\tilde{\beta}}e^{i\Gamma_{\gamma_p}^{\tilde{\beta}}}$ is given by the product over r in Eq. (43). The sum is over clockwise and counterclockwise propagating POs. Reversing the rotational direction of the PO corresponds to swapping the sign of χ_r in Eq. (43), turning $\mathcal{B}_{\gamma_p}^{\tilde{\beta}}e^{i\Gamma_{\gamma_p}^{\tilde{\beta}}}$ into an, in general different term which we denote by $\tilde{\mathcal{B}}_{\gamma_p}^{\tilde{\beta}}e^{i\tilde{\Gamma}_{\gamma_p}^{\tilde{\beta}}}$. Furthermore, Φ_{γ_p} turns into $\tilde{\Phi}_{\gamma_p}=-\Phi_{\gamma_p}$, whereas the factors from Gutzwiller's trace formula do not change. Consequently, the contributions of the clockwise and counterclockwise propagating orbits differ for NBs, that is, they exhibit the chirality property. The real part of the summands in Eq. (49) becomes

$$\begin{aligned}2\mathcal{P}_{\gamma_p}^{\tilde{\beta}}=&\mathcal{B}_{\gamma_p}^{\tilde{\beta}}\cos\left(\Phi_{\gamma_p}-p\frac{\pi}{2}\right)\cos\left(\Theta_{\gamma_p}+\Gamma_{\gamma_p}^{\tilde{\beta}}\right)\\&+\tilde{\mathcal{B}}_{\gamma_p}^{\tilde{\beta}}\cos\left(\Phi_{\gamma_p}+p\frac{\pi}{2}\right)\cos\left(\Theta_{\gamma_p}+\tilde{\Gamma}_{\gamma_p}^{\tilde{\beta}}\right)\end{aligned} \tag{51}$$

$$\begin{aligned}=&\cos\left(\Phi_{\gamma_p}-p\frac{\pi}{2}\right)\\&\times\left[\mathcal{B}_{\gamma_p}^{\tilde{\beta}}\cos\left(\Theta_{\gamma_p}+\Gamma_{\gamma_p}^{\tilde{\beta}}\right)+(-1)^p\tilde{\mathcal{B}}_{\gamma_p}^{\tilde{\beta}}\cos\left(\Theta_{\gamma_p}+\tilde{\Gamma}_{\gamma_p}^{\tilde{\beta}}\right)\right].\end{aligned} \tag{52}$$

We finally obtain for the trace formula of massive neutrino billiards

$$\rho^{\mathrm{fluc}}(k;\tilde{\beta})=\frac{1}{\pi}\sum_{p}\sum_{\gamma_p}\mathcal{A}_{\gamma_p}\mathcal{P}_{\gamma_p}^{\tilde{\beta}}. \tag{53}$$

In the massless, i.e., the ultrarelativistic case $\beta=0$ and $\theta_\beta=0$ so that $\mathcal{B}_{\gamma_p}^{\tilde{\beta}}e^{i\Gamma_{\gamma_p}^{\tilde{\beta}}}=(-1)^p$ and

$$\mathcal{P}_{\gamma_p}^{\tilde{\beta}}\xrightarrow{\beta\to0}(-1)^p 2\cos\left(\Phi_{\gamma_p}\right)\cos\left(p\frac{\pi}{2}\right)\cos\left(\Theta_{\gamma_p}\right). \tag{54}$$

Thus, the trace formula for massless NBs differs from that of QBs by the product of the first two cosine functions which vanishes for odd p, implying that only POs with an even number of reflections at the boundary [39,51] contribute to it. This difference has its origin in the chirality property and the additional spin degree of freedom. Actually, a similar behavior was observed in Refs. [71,72] for three-dimensional microwave resonators where it can be attributed to the vectorial character of the Helmholtz equation. Generally, for $\beta\to0$ contributions of POs with odd periodicity p are negligible. Yet, for nonzero mass, i.e., $\theta_\beta\neq0$ the second term in the curly brackets of Eq. (43) yields a nonvanishing contribution of POs with an odd number of reflections.

In the nonrelativistic limit $\beta\to\infty$, that is, $\theta_\beta\to\frac{\pi}{2}$, Eq. (43) becomes

$$\mathcal{B}_{\gamma_p}^{\tilde{\beta}}e^{i\Gamma_{\gamma_p}^{\tilde{\beta}}}\xrightarrow{\beta\to\infty}\prod_{r=1}^{p}\{ie^{-i\frac{\chi_r+\chi_{r+1}}{2}}\}=e^{i[p\frac{\pi}{2}-\Phi_{\gamma_p}]}, \tag{55}$$

yielding

$$\begin{aligned}2\mathcal{P}_{\gamma_p}^{\tilde{\beta}}\xrightarrow{\beta\to\infty}&\cos\left(\Phi_{\gamma_p}-p\frac{\pi}{2}\right)\left\{\cos\left(\Theta_{\gamma_p}-\left[\Phi_{\gamma_p}-p\frac{\pi}{2}\right]\right)\right.\\&\left.+(-1)^p\cos\left(\Theta_{\gamma_p}-\left[\Phi_{\gamma_p}+p\frac{\pi}{2}\right]\right)\right\}\\=&2\cos\left(\Phi_{\gamma_p}-p\frac{\pi}{2}\right)\cos\left(\Theta_{\gamma_p}-\left[\Phi_{\gamma_p}-p\frac{\pi}{2}\right]\right)\\\equiv&2\cos\left(\Theta_{\gamma_p}\right),\end{aligned} \tag{56}$$

where we used the fact that $\Phi_{\gamma_p} - p\frac{\pi}{2}$ is a multiple of π; see Eq. (48). Thus, in the nonrelativistic limit the trace formula for a massive NB Eq. (53) turns into Gutzwiller's trace formula for the corresponding QB given in Eq. (41).

VI. TRACE FORMULA FOR A MASSIVE CIRCULAR NB

We mentioned above that we used a combination of Eqs. (18) and (26) to obtain a trace formula with convergence properties similar to those of Gutzwiller's trace formula. This is the case in the limits $\theta_\beta \to 0$ and $\theta_\beta \to \pi/2$, respectively, where the product $\tilde{\mathcal{P}}_p^*$ in Eq. (43) is proportional to the denominator of the last term in Eq. (38). However, in the intermediate region $0 < \theta_\beta < \pi/2$ convergence problems might arise due to the $\cos\theta_\beta$ term in the curly brackets of Eq. (43) which does not factorize into a product of $\cos(\alpha_r - \xi_{r+1,r}) = -\cos\chi_r$ multiplied with a term which is nonsingular at $\chi_r \simeq \pi/2$; see Eq. (B13) of Appendix B. Thus it becomes large for POs which are nearly tangential to the boundary in some parts. Examples for such orbits are whispering-gallery-type POs in billiards with a circular shape with lengths close to a multiple of the circumference of the billiard [63] or in the stadium billiard [62,73]. In order to study the convergence properties of the trace formula Eq. (53), we first considered the massive circular NBs, also to test whether, like in the nonrelativistic [63] and the ultrarelativistic case [54], the derivation used to derive the trace formula also applies to massive NBs with the shape of an integrable CB. Another reason is that the eigenstates are known analytically. They are obtained for a circular NB of radius $\mathcal{R}$ by solving Eq. (10) with the BC Eq. (11) in polar coordinates (r,ϕ) where $r \in [0,\mathcal{R}]$ and $\phi \in [0, 2\pi)$ [67], yielding

$$\tilde{\psi}_{1,m}(r,\phi) = a_m i^m J_m(kr) e^{im\phi}, \tag{57}$$

$$\tilde{\psi}_{2,m}(r,\phi) = a_m i^{m+1} J_{m+1}(kr) e^{i(m+1)\phi}, \tag{58}$$

and thus $\psi_{1,m}(r,\phi)$ and $\psi_{2,m}(r,\phi)$ with Eq. (9). Using orthogonality along the boundary yields with the BC Eq. (11) the quantization condition

$$J_{m+1}(k\mathcal{R}) = \mathcal{K}^{-1} J_m(k\mathcal{R}). \tag{59}$$

We set $\mathcal{R} = 1$ cm in the following.

For a circular billiard the angles of reflection χ_r of a PO are all equivalent and are given for a PO with p reflections at the boundary and winding number m_φ by

$$\chi_r = \left[\frac{\mathrm{sgn}(m_\varphi)}{2} - \frac{m_\varphi}{p}\right]\pi, \quad r = 1,\ldots,p, \tag{60}$$

where $\mathrm{sgn}(m_\varphi) = \pm 1$ for clockwise and counterclockwise POs, respectively, so that

$$\mathcal{B}_{\gamma_p}^{\tilde{\beta}} e^{i\Gamma_{\gamma_p}^{\tilde{\beta}}} = \left[-\cos\theta_\beta + i\sin\theta_\beta \sin\left(\pi\frac{|m_\varphi|}{p}\right)\right]^p \times \left[1 \pm i\sin\theta_\beta \cot\left(\pi\frac{|m_\varphi|}{p}\right)\right]^p \tag{61}$$

and

$$\cos\left(\Phi_{\gamma_p} - p\frac{\pi}{2}\right) = \cos\left(\left[m_\varphi - \frac{p}{2} \pm \frac{p}{2}\right]\pi\right). \tag{62}$$

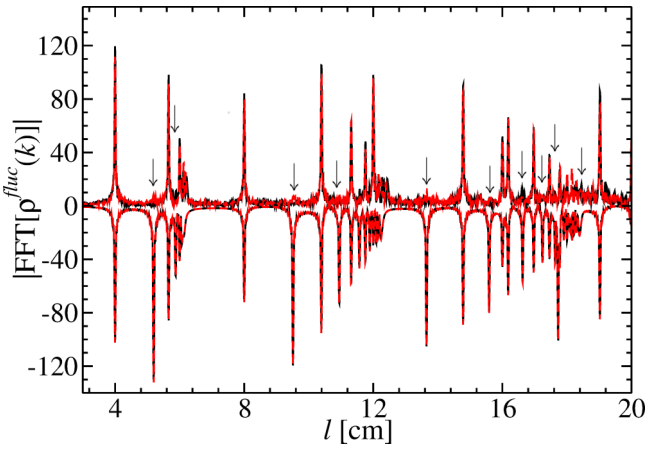

FIG. 2. Comparison of the length spectrum deduced from the eigenvalues of the circular NB (black dots and line) for the ultrarelativistic limit $\tilde{\beta} = 0$ (upper part) with that obtained from the Fourier transform of the associated trace formula Eq. (53) from k to l (red dots and line). To illustrate cancellation of POs with odd periodicity we compare them with those for the nonrelativistic QB (lower part). The arrows point at the lengths of POs with an odd number of reflections.

In the rest of the paper we restrict to $m_\varphi > 0$. Furthermore, for the circular billiard

$$\mathcal{A}_{\gamma_p} e^{i\Theta_{\gamma_p}} = \sqrt{\frac{k}{\pi}}(2-\delta_{p,2m_\varphi}) \frac{\left(\sin\frac{m_\varphi}{p}\pi\right)^{3/2}}{\sqrt{p}} e^{i[2kp\sin(\frac{m_\varphi}{p}\pi) - \frac{3\pi}{2}p + \frac{\pi}{4}]}. \tag{63}$$

Using the quantization condition Eq. (59), we computed the eigenstates of massive circular NBs for several values of $\tilde{\beta}$ below $k\mathcal{R} = 200$ yielding ≈10 000 eigenvalues for each of them. Here we use the fact that NBs are scale invariant, that is, $\hbar$ can be set, e.g., to $\hbar = 1$. We compared their length spectra, that is, the modulus of the Fourier transform of $\rho^{\mathrm{fluc}}(k;\tilde{\beta})$ from k to length l, to those deduced from the associated trace formula. In the upper part of Fig. 2 we show the length spectrum for the ultrarelativistic case $\tilde{\beta} = 0$ obtained from the eigenvalues (black lines) with that obtained from the corresponding trace formula (red dashed line) and in the lower part those for the nonrelativistic QB. Lengths corresponding to POs with an odd number of reflections at the boundary are marked by arrows. It is clearly visible that these are missing in the length spectrum of the massless NB.

The contribution of the $\cos\theta_\beta$ term to $\mathcal{B}_{\gamma_p}^{\tilde{\beta}} e^{i\Gamma_{\gamma_p}^{\tilde{\beta}}}$ in Eq. (61) becomes large for $\frac{m_\varphi}{p} \simeq 0$, that is, for whispering-gallery modes with lengths close to $2\pi\mathcal{R}$ after one loop of the PO and might result in convergence problems in the numerical analysis depending on the value of $2\sin\theta_\beta\cos\theta_\beta = \sin(2\theta_\beta)$ beyond a certain value of p in Eq. (60) if these contributions do not interfere destructively with other POs, or the contributions for clockwise and counterclockwise POs do not cancel each other. To control convergence we set an upper limit on the size of $|\cos\chi_r| \geqslant \epsilon$ which corresponds to disregarding the contributions of POs with reflection angles above a certain value and compared the resulting fluctuating part $N^{\mathrm{fluc}}(k;\tilde{\beta})$ of the integrated spectral density deduced from the eigenvalues of massive NBs with

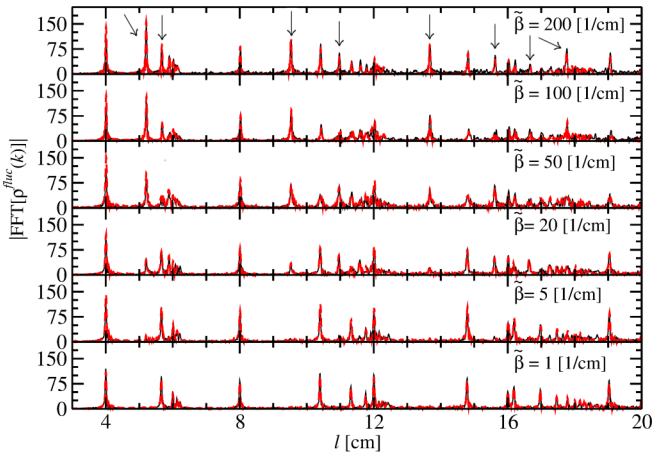

FIG. 3. Comparison of the length spectra deduced from the eigenvalues of massive circular NB (black lines) with those obtained by integrating the associated trace formula Eq. (53) (see main text) over k (red dashed lines). The values of $\tilde{\beta}$ are given in the panels. The arrows point at the lengths of POs with an odd number of reflections.

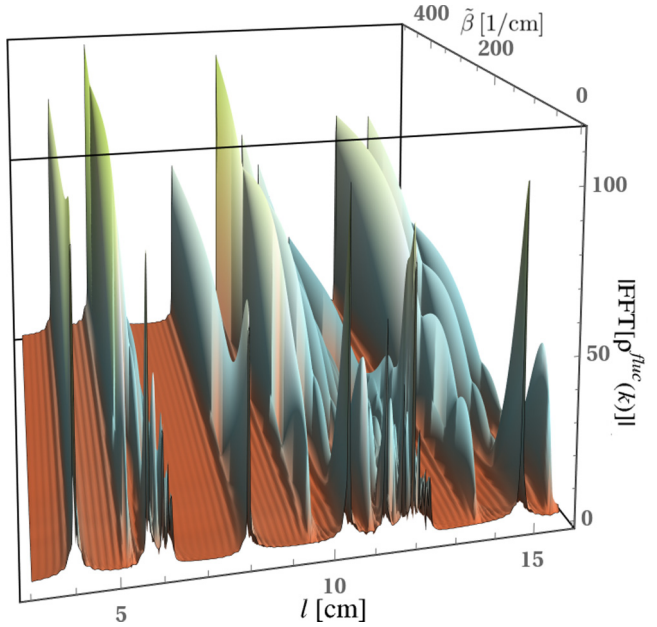

FIG. 4. Evolution of the length spectrum with $\tilde{\beta}$ of the massive circular NB obtained from the Fourier transform of the trace formula Eq. (53) over k (red dots and line) for $3 \leqslant \tilde{\beta} \leqslant 15.8$/cm and $0 \leqslant \tilde{\beta} \leqslant 500$/cm.

$\tilde{\beta} = 0.5, 1, 2, 5, 10, 20, 50, 75, 100, 200$/cm with that obtained by integrating the associated trace formula over k for lengths below $l = 20$ cm. Generally, more sophisticated approaches are available to achieve convergence of the trace formula depending on the demands [63,74,75]. However, this goes beyond the scope of the present article. It turned out, that for $k\mathcal{R} \leqslant 200$ the nonrelativistic limit is reached for $\tilde{\beta} \approx 500$/cm. In Fig. 3 we show a few examples. The peaks at $l = 4, 8, 16$ cm, which correspond to the diameter orbit and repetitions of it barely change with $\tilde{\beta}$, whereas that at $l = 12$ cm changes height with $\tilde{\beta}$. This may be attributed to an interference with orbits accumulating in its vicinity. Furthermore, the heights of peaks at lengths corresponding to POs with an odd number of reflections at the boundary, marked by arrows, partly increase with increasing $\tilde{\beta}$, whereas others oscillate in height when changing θ_β. Above $l = 16$ cm it is difficult to distinguish these POs in the region where POs accumulate. The evolution of the length spectrum with increasing $\tilde{\beta}$ is illustrated in Fig. 4.

VII. TRACE FORMULA FOR A CONSTANT WIDTH NB

We computed POs up to a length of 150 cm for the constant width (CW) billiard with the shape of the microwave billiard studied experimentally in Ref. [28]. The shape is illustrated in Fig. 1. The boundary coordinates $\boldsymbol{r}(s) = [x(s), y(s)]$ are obtained as the real and imaginary parts of $w(s) = x(s) + iy(s)$, where

$$w(s) = -ia_0 - i\sum_{n\in\mathbb{Z}} \frac{a_n}{n+1}[e^{i(n+1)\alpha} - 1],\ \alpha \in [0, 2\pi) \quad (64)$$

and $a_{-n} = a_n^*$, $a_1 = 0$, $a_{2n} = 0$ for $n \geqslant 1$, and $a_{2n+1} = 0$ for $n \geqslant 3$. The radius equaled $\mathcal{R} = a_0 = 12$ cm, $a_3 = \frac{3}{2}i$ cm, and $a_5 = 3$ cm. It exhibits a unidirectional dynamic, that is, the change of the rotational direction of motion from clockwise to counterclockwise is not possible. Accordingly, its Poincaré surface of section (PSOS) depicted in Fig. 5 consists of two parts that are well separated by a barrier region of Kolmogorov-Arnold-Moser tori [26,27,76–78] around the diameter orbit. In each part the classical dynamic is predominantly chaotic except for tiny islands of regular motion in the PSOS corresponding to a PO with 11 reflections and length $l_{\mathrm{PO}} = 76.83$ cm, whispering-gallery orbits and the region around the diameter orbit. Although the transition through the barrier is forbidden in the classical system, it occurs in the corresponding QB due to dynamical tunneling. This becomes manifest in the splitting of the vast majority of eigenstates into doublets of nearly degenerate ones [28,76]. The separation into doublet partners was not possible in the CW NB. A similar result was found for the unidirectional Monza billiard [67], indicating that dynamical tunneling is stronger in the NB than in the corresponding nonrelativistic QB.

We computed 5000 eigenvalues for the massless CW NB using Eq. (18) for $\theta_\beta = 0$ and for the corresponding QB using the associated BIEs [68], that is, for $k\mathcal{R} \lesssim 12$. In Fig. 6 we compare $N^{\mathrm{fluc}}(k;\tilde{\beta})$ for the massless NB, deduced from the eigenvalues (black dots and lines) with that computed from the trace formula (53) (red dots and dashed lines). It exhibits fast fluctuations and slow oscillations where the latter are due to the diameter orbit. The associated eigenstates correspond to those of the circular NB of the same radius [28]. Accordingly, their contribution to $\rho^{\mathrm{fluc}}(k;\tilde{\beta})$ is obtained from the trace formula derived in Sec. VI. For the diameter orbits we have $p = 2|m_\varphi|$ in Eqs. (61)–(63), yielding

$$\begin{aligned}\rho^{\mathrm{diam}}(k;\tilde{\beta}) &= \sqrt{\frac{k\mathcal{R}}{\pi}}\mathrm{Re}\sum_p \frac{[1+(-1)^p]}{2}(-1)^{3p/2}e^{-ip\theta_\beta}\frac{e^{i[2kp\mathcal{R}-\frac{3\pi}{2}p+\frac{\pi}{4}]}}{\sqrt{p}} \\ &= \sqrt{\frac{k\mathcal{R}}{\pi}}\sum_{p\,\mathrm{even}}\frac{\cos\left(2kp\mathcal{R}-p\theta_\beta+\frac{\pi}{4}\right)}{\sqrt{p}}. \end{aligned} \quad (65)$$

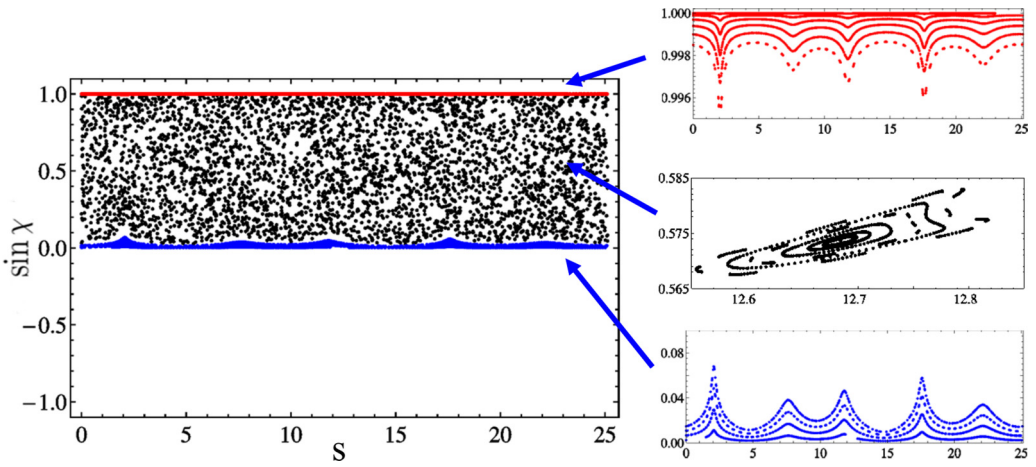

FIG. 5. Poincaré surface of section for the constant-width billiard. It was generated by launching particles into the billiard in clockwise direction. The chaotic sea is framed by a region of whispering-gallery modes around $\chi = \pm\pi/2$ and a region around the diameter orbit at $\chi = 0$. Furthermore, it contains tiny islands in the chaotic sea which correspond to a PO with 11 reflections and a length of 76.83 cm. Here χ denotes the reflection angle with respect to the outward pointing normal at the boundary.

The fluctuating part of the integrated spectral density deduced from it is plotted as turquoise dashed line in Fig. 6. The agreement of the three curves is very good. Note, that this comparison provides a stringent test for the validity of the semiclassical quantization.

To illustrate cancellation of POs of odd periodicity we compare in Fig. 7 length spectra of the massless CW NB (upper part) and the corresponding QB (lower part) [28], namely, only peaks at lengths which correspond to POs with an even number of reflections are observed in that of the NB. Deviations are visible especially for the length spectrum of the QB [28] at the length $l = 76.83$ cm (middle arrow in Fig. 7 of the PO corresponding to the small regular islands in the chaotic sea [28] and at the $l \simeq 69.31$ cm and $l \simeq 138.63$ cm (left and right arrow in Fig. 7), respectively, corresponding to whispering-gallery modes. These orbits are not accounted for in Gutzwiller's trace formula and accordingly also not in its analog for NBs given in Eq. (53). The turquoise dashed curves are obtained from the trace formula Eq. (65) for the diameter orbit. At the peaks corresponding to this orbit and its repetitions all curves lie on top of each other.

In order to check the validity of the trace formula Eq. (53) in the intermediate region, we computed 1500 eigenvalues for several values of $\tilde{\beta}$ using Eq. (19) and compared the resulting fluctuating part of $N^{\rm fluc}(k;\tilde{\beta})$ and length spectra with those deduced from Eq. (53). The determination of the eigenvalues becomes more and more cumbersome with increasing $\tilde{\beta}$, since

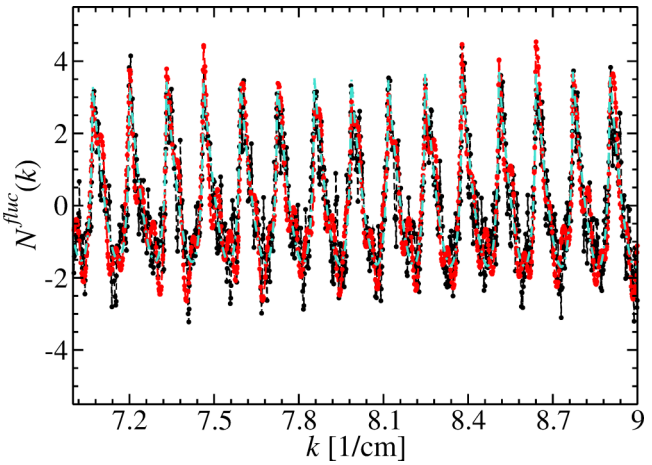

FIG. 6. Comparison of the fluctuating part of the integrated spectral density deduced from the eigenvalues of the massless constant-width NB (black dots and line) with that obtained by integrating the associated trace formula Eq. (53) over k (red dots and line) and from that for the diameter orbit Eq. (65) (turquoise).

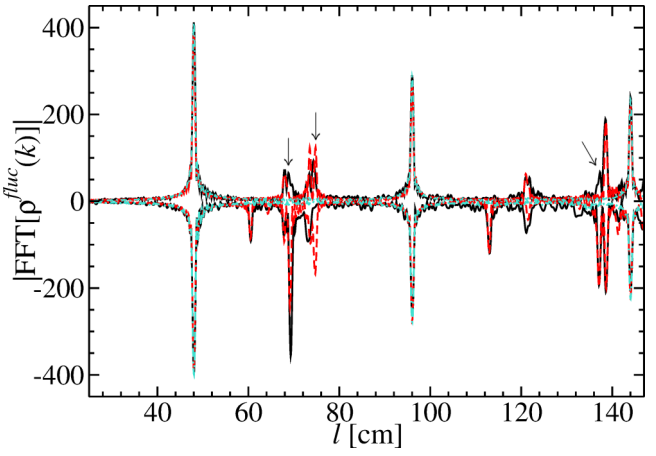

FIG. 7. Comparison of the length spectrum deduced from the eigenvalues of the massless constant-width NB (black dots and line) (upper part) with that obtained from the Fourier transform of the associated trace formula Eq. (53) from k to l (red dots and line) and from that for the diameter orbit Eq. (65) (turquoise). To illustrate cancellation of POs with odd periodicity we compare the length spectrum for the ultrarelativistic case $\tilde{\beta} = 0$ with that for the non-relativistic limit $\tilde{\beta} \to \infty$ (lower part). The left and right arrows point at the lengths of whispering-gallery modes and the middle one at the length of the PO corresponding to the tiny regular islands in the chaotic sea.

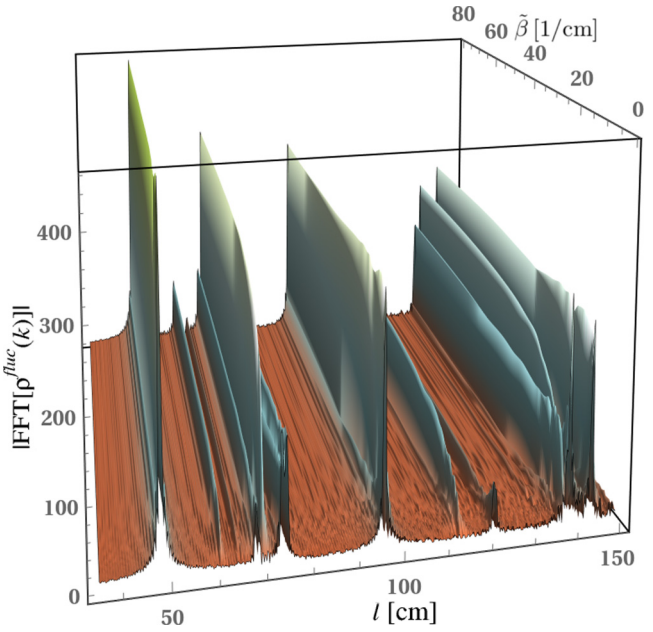

FIG. 8. Length spectrum of the massive CW NB obtained from the Fourier transform of the trace formula Eq. (53) over k (red dots and line) for $0 \leqslant \tilde{\beta} \leqslant 60/\mathrm{cm}$.

pairs of eigenvalues approach each other. We will report on the spectral properties of CW NB in a forthcoming publication.

Note that the trace formula applies to POs within the chaotic sea in Fig. 5 which implies that the reflection angle with respect to the normal vector to the boundary is $\chi < \pi/2$ so that whispering-gallery-type modes do not contribute to Eq. (43) [73]. We checked that the agreement between the numerical and semiclassical results is as good as for the massless NB and the QB. For this one needs to make sure that whispering-gallery type POs, especially those with lengths corresponding to a multiple of the length of the circumference, which, actually, is close to that of the PO associated with the small islands in the chaotic sea [28], $l = 75.40$ cm, are deleted in the list of POs. In Fig. 8 we show the transition of the length spectrum from the ultrarelativistic to the nonrelativistic limit. The peaks corresponding to the diamater orbit at 48 cm and its repetitions barely increase in height, and those corresponding to POs with an odd number of reflections increase smoothly from zero to the height they attain in the nonrelativistic limit, which is reached for $\tilde{\beta} \simeq 80/\mathrm{cm}$. On the other hand, peaks of which the positions are close to the lengths of integrable PO or whispering-gallery-type POs first decay rapidly when increasing $\tilde{\beta}$ and then increase slowly. This maybe attributed to nonchaotic POs [62], of which, in fact, the effect on the length spectra is particularly large for the massless NB as may be concluded from the results for the ultrarelativistic and nonrelativistic limits.

VIII. CONCLUSIONS

We derive BIEs for massive neutrino billiards and deduce from them a semiclassical quantization condition in terms of a spectral determinant. The latter provides the starting point for the derivation of a trace formula, which undergoes a transition from that for NBs for massless spin-1/2 particles [54] to that for nonrelativistic QBs [19,56,57] when increasing mc. In the ultrarelativistic limit only POs with an even number of reflections at the boundary contribute to it. The relevant parameter for the transition to the nonrelativistic case is the ratio β of the rest-energy momentum mc and free-space momentum $\hbar k$, implying that the result Eq. (54) for massless NBs is also approached for massive NBs with rest-mass momentum mc when increasing the free-space momentum $\hbar k$ such that $\beta \to 0$, that is, in the high-energy limit. For massive NBs, that is, $0 < \theta_\beta$, the second term in Eq. (43) leads to an incomplete cancellation of clockwise and counterclockwise contributions for odd p, implying that also POs with an odd number of reflections at the boundary contribute to the trace formula.

We note that a trace formula for NBs can also be obtained by proceeding as in Ref. [39], where trace formulas were derived for finite-size graphene nanostructures, referred to as graphene billiards [43,50], with various edge types including infinite-mass confinement. There, a boundary matrix was introduced in spinor space to formulate the BC as a matrix equation $\boldsymbol{P}_s \boldsymbol{\psi}^* = 0$, which for the BC Eq. (10) takes the form

$$\boldsymbol{P}_{s_r} = \frac{1}{2}\begin{pmatrix} 1 & ie^{i\alpha_r}\mathcal{K} \\ -ie^{-i\alpha_r}\mathcal{K}^{-1} & 1 \end{pmatrix}. \tag{66}$$

The trace formula derived in Ref. [39] also differs from Gutzwiller's trace formula by an additional factor and is obtained from Eq. (50) by replacing the factor $2\cos(\Phi_{\gamma_p} - p\frac{\pi}{2})\mathcal{B}^{\tilde{\beta}}_{\gamma_p} e^{i\Gamma^{\tilde{\beta}}_{\gamma_p}}$ by

$$\mathrm{Tr}(K_\gamma) = \mathrm{Tr}\left\{\prod_r \mathcal{O}_{r,r-1}\frac{-1}{\cos[\xi_{r,r-1} - \alpha_r]}\right\}, \tag{67}$$

where

$$\mathcal{O}_{r,r-1} = \left[\mathbb{1} + \hat{\boldsymbol{\sigma}} \cdot \frac{\boldsymbol{r}(s_r) - \boldsymbol{r}(s_{r-1})}{\rho(s_r, s_{r-1})}\right][\hat{\boldsymbol{\sigma}} \cdot \boldsymbol{n}(s_r)]\boldsymbol{P}_{s_r} \tag{68}$$

$$= \begin{pmatrix} 1 & e^{i\xi_{r,r-1}} \\ e^{-i\xi_{r,r-1}} & 1 \end{pmatrix}\begin{pmatrix} 0 & e^{i\alpha_r} \\ e^{-i\alpha_r} & 1 \end{pmatrix} \times \begin{pmatrix} 0 & ie^{i\alpha_r}\mathcal{K} \\ -ie^{-i\alpha_r}\mathcal{K}^{-1} & 1 \end{pmatrix}$$

$$= \begin{bmatrix} e^{i(\xi_{r,r-1}-\alpha_r)} - i\mathcal{K}^{-1} & e^{i\alpha_r} + i\mathcal{K}e^{i\xi_{r,r-1}} \\ e^{-i\alpha_r} - i\mathcal{K}^{-1}e^{-i\xi_{r,r-1}} & e^{-i(\xi_{r,r-1}-\alpha_r)} + i\mathcal{K} \end{bmatrix}. \tag{69}$$

The matrix $\mathcal{O}_{r,r-1}$ coincides with that obtained from Eqs. (12) and (13) with Eq. (35) after discretizing them,

$$\boldsymbol{\psi}(s_r) \simeq \mathcal{O}_{r,r-1}\boldsymbol{\psi}(s_{r-1})H_1^{(1)}[k\rho(s_r, s_{r-1})]. \tag{70}$$

It was demonstrated in Ref. [54] that the trace formulas for infinite-mass confinement in a circular graphene billiard and for a massless circular NB coincide. The difference between the approach of Ref. [39] and ours is, that we start from BIEs deduced from Eqs. (12) and (13) which do not contain singularities, and a large-k approximation of the BIEs obtained from the BC Eq. (3). The advantage of our approach is that the phase factor can be computed explicitly and thus the convergence problems of the resulting trace formula, that might occur for the finite-mass case, can be controlled. The result is a closed expression in terms of the phase accumulated during each path of a p-periodic loop and revealing the property that

orbits with an odd periodicity are increasingly suppressed for $\theta_\beta \to 0$, which interpolates between the ultrarelativistic and the nonrelativistic limits.

A motivation for the studies of the present article is the search for boundary conditions which yield a good description of the length spectra and spectral properties obtained experimentally with superconducting microwave billiards in Refs. [43,44] emulating artificial graphene. The experimental length spectra exhibited deviations from those deduced based the trace formula for graphene billiards with infinite-mass confinement [39]. Further detailed studies based on the results for massive NBs, that is, for relativistic billiards with varying BCs, will be performed.

ACKNOWLEDGMENT

This work was supported by NNSF of China under Grants No. 11775100 and No. 11961131009. Furthermore, we thank Martin Sieber for fruitful discussions.

APPENDIX A: BOUNDARY INTEGRAL FOR A MASSIVE CIRCULAR NEUTRINO BILLIARD

We compute the eigenstates based on the BIEs Eq. (18) where the arc-length parameter is given as $s = \phi \in [0, 2\pi)$, $\boldsymbol{r}(\phi) = R(\cos\phi, \sin\phi)$ defines the boundary and $e^{i\alpha} = e^{i\phi}$ [54] so that Eq. (18) becomes

$$\psi_1^\star(\phi') = \frac{i}{4}k\int_0^{2\pi} \mathcal{R}d\phi \times \left\{\mathcal{K}e^{i(\phi'-\phi)} - \mathcal{K}^{-1}\right\}H_0^{(1)}\left[2k\mathcal{R}\left|\sin\left(\frac{\phi-\phi'}{2}\right)\right|\right]\psi_1^\star(\phi). \tag{A1}$$

As in Ref. [54] we choose as ansatz for the boundary function at $r = \mathcal{R}$ an expansion in terms of plane waves,

$$\psi_1^\star(\phi) = \sum_l a_l i^l J_l(k\mathcal{R})e^{-il\phi}, \tag{A2}$$

$$\psi_2^\star(\phi) = \sum_l a_l i^{l+1} J_{l+1}(k\mathcal{R})e^{-i(l+1)\phi}, \tag{A3}$$

yielding with the notation $\tilde\phi = \phi' - \phi$,

$$\sum_l a_l i^l J_l(k\mathcal{R})e^{-il\phi'} = \sum_l a_l i^l J_l(k\mathcal{R})e^{-il\phi'} \times \frac{ik}{4}\mathcal{R}\int_0^{2\pi} d\tilde\phi\{\mathcal{K}e^{i\tilde\phi} - \mathcal{K}^{-1}\}e^{il\phi}H_0^{(1)}\left(2k\mathcal{R}\left|\sin\frac{\tilde\phi}{2}\right|\right). \tag{A4}$$

The integral over ϕ can be performed,

$$\int_0^{2\pi} d\tilde\phi[\mathcal{K}e^{i(l+1)\tilde\phi} - \mathcal{K}^{-1}e^{il\tilde\phi}]H_0^{(1)}\left(2k\mathcal{R}\left|\sin\frac{\tilde\phi}{2}\right|\right) = 2\pi\left[\mathcal{K}J_{l+1}^2(k\mathcal{R}) - \mathcal{K}^{-1}J_l^2(k\mathcal{R})\right] + 2\pi i[\mathcal{K}J_{l+1}(k\mathcal{R})Y_{l+1}(k\mathcal{R}) - \mathcal{K}^{-1}J_l(k\mathcal{R})Y_l(k\mathcal{R})].$$

Multiplying Eq. (A4) with $e^{im\phi'}$ and performing the integral over ϕ' leads to component-by-component equations for the real and imaginary part, respectively, which have solutions at discrete values of k. We obtain for the latter

$$0 = \mathcal{K}J_{m+1}^2(k\mathcal{R}) - \mathcal{K}^{-1}J_m^2(k\mathcal{R}), \tag{A5}$$

that is,

$$J_m(k\mathcal{R}) = \pm\mathcal{K}J_{m+1}(k\mathcal{R}). \tag{A6}$$

and for the real part with Eq. (A6),

$$\begin{aligned} 1 &= \frac{\pi k\mathcal{R}}{2}[\mathcal{K}^{-1}J_m(k\mathcal{R})Y_m(k\mathcal{R}) - \mathcal{K}J_{m+1}(k\mathcal{R})Y_{m+1}(k\mathcal{R})] \\ &= \pm\frac{\pi k\mathcal{R}}{2}[J_{m+1}(k\mathcal{R})Y_m(k\mathcal{R}) - J_m(k\mathcal{R})Y_{m+1}(k\mathcal{R})] \\ &= \pm 1. \end{aligned}$$

Here the term in rectangular brackets in the second line is the Wronskian $W\{J_m(k\mathcal{R}), Y_m(k\mathcal{R})\} = \frac{2}{\pi k\mathcal{R}}$. Thus Eq. (A1) is fulfilled for

$$J_m(k_n\mathcal{R}) = \sqrt{\frac{\sqrt{(\hbar k_n)^2 + (mc)^2} - \hbar k_n}{\sqrt{(\hbar k_n)^2 + (mc)^2} + \hbar k_n}}J_{m+1}(k_n\mathcal{R}). \tag{A7}$$

This yields the eigenwave numbers k_n, $n = 1, 2, \ldots$. The eigenvalues $E_n = \hbar c k_{E,n}$ are obtained as $k_{E,n} = \sqrt{k_n^2 + \tilde\beta^2}$ with $\tilde\beta = \frac{mc}{\hbar}$.

APPENDIX B: EQUATIONS RELEVANT FOR THE DERIVATION OF THE TRACE FORMULA

The integral equation used to remove the logarithmic singulartiy in Eq. (18) is obtained by imposing on $\tilde\psi_1(s')$ and $\tilde\psi_2(s')$ the BC Eq. (11) using the right-hand sides of Eqs. (12) and (13). This leads to the integral equation

$$\begin{aligned} &\oint_{\partial\Omega} ds e^{i\frac{\Delta\Phi(s,s')}{2}}\tilde\psi_1^*(s)\cos\left[\frac{\Delta\Phi(s,s')}{2}\right]\frac{ik}{4}H_0^{(1)}(k\rho) \\ &= \oint_{\partial\Omega} ds e^{i\frac{\Delta\Phi(s,s')}{2}} i\tilde\psi_1^*(s) \\ &\quad\times\left\{\sin\theta_\beta\sin\left[\frac{\Delta\Phi(s,s')}{2}\right]\frac{ik}{4}H_0^{(1)}(k\rho)\right. \\ &\quad\left. - \cos\theta_\beta\sin\left[\frac{\alpha(s')+\alpha(s)}{2} - \xi(s,s')\right]\frac{ik}{4}H_1^{(1)}(k\rho)\right\}. \end{aligned} \tag{B1}$$

Equation (26) is derived from the boundary condition Eq. (11). To obtain it we used the following equations for the normal and tangential derivatives,

$$\partial_{n'}H_0^{(1)}[k\rho(s,s')] = \cos[\xi(s,s') - \alpha(s')] \times kH_1^{(1)}[k\rho(s,s')], \tag{B2}$$

$$\partial_{n'}H_1^{(1)}[k\rho(s,s')] = \cos[\xi(s,s') - \alpha(s')] \times k\left\{\frac{H_1^{(1)}[k\rho(s,s')]}{k\rho(s,s')} - H_0^{(1)}[k\rho(s,s')]\right\}, \tag{B3}$$

$$\partial_{s'} H_0^{(1)}[k\rho(s,s')] = \sin[\xi(s,s') - \alpha(s')] k H_1^{(1)}[k\rho(s,s')], \tag{B4}$$

$$\partial_{s'} H_1^{(1)}[k\rho(s,s')] = \sin[\xi(s,s') - \alpha(s')] \times k\left\{\frac{H_1^{(1)}[k\rho(s,s')]}{k\rho(s,s')} - H_0^{(1)}[k\rho(s,s')]\right\}, \tag{B5}$$

$$\partial_{n'} e^{i\xi(s,s')} = i \sin[\xi(s,s') - \alpha(s')] \frac{e^{i\xi(s,s')}}{\rho(s,s')}, \tag{B6}$$

$$\partial_{s'} e^{i\xi(s,s')} = -i \cos[\xi(s,s') - \alpha(s')] \frac{e^{i\xi(s,s')}}{\rho(s,s')}. \tag{B7}$$

Applying these equations to Eqs. (12) and (13) yields that the wave-function components $\psi_{1,2}(\boldsymbol{r})$ indeed fulfill the boundary conditions Eq. (3).

The starting point for the derivation of the BIE Eq. (26) is the BC Eq. (11) which provides a relation between the normal derivatives of $\Phi_{1,2}$ and the wave-function components, that is, we need to determine the normal derivatives of the BIEs Eq. (12) and Eq. (13). For this we use Eq. (3) to compute the tangential derivatives instead of the normal derivatives and also directly compute the normal derivatives and compare results to ensure that any jump relations for the normal derivatives [79] are accounted for. We have from Eq. (3),

$$-\frac{k}{2}\left[\mathcal{K}^{-1} - \mathcal{K} + \frac{\kappa(s')}{k}\right] \tag{B8}$$

$$\begin{aligned}
&= \frac{\partial_{n'}\psi_1^*(s') + ie^{i\alpha(s')}\partial_{n'}\psi_1^*(s')}{2} \\
&= \frac{i\partial_{s'}\psi_1^*(s') - ie^{i\alpha(s')} i\partial_{s'}\psi_1^*(s')}{2} + k\frac{[\mathcal{K}^{-1} - \mathcal{K}]}{2} \\
&= \frac{ik}{4}\oint_{\partial\Omega} ds \psi_1^*(s) \\
&\quad \times \left\{[\mathcal{K} e^{i[\alpha(s') - \alpha(s)]} + \mathcal{K}^{-1}] k H_1^{(1)}[k\rho(s,s')] \right. \\
&\quad \left. - [e^{i[\xi(s,s') - \alpha(s)]} + e^{i[\alpha(s') - \xi(s,s')]}] k H_0^{(1)}[k\rho(s,s')]\right\} \\
&\quad \times \cos[\xi(s,s') - \alpha(s')] \\
&\quad + \frac{ik}{4}\oint_{\partial\Omega} ds \psi_1^*(s)\left\{[e^{i[\alpha(s') - \alpha(s)]} + 1] k H_0^{(1)}[k\rho(s,s')] \right. \\
&\quad \left. - [\mathcal{K} e^{i[\alpha(s') - \alpha(s)]} + \mathcal{K}^{-1}] e^{i[\xi(s,s') - \alpha(s')]} k H_1^{(1)}[k\rho(s,s')]\right\} \\
&\quad + \frac{ik}{4}\oint_{\partial\Omega} ds \psi_1^*(s) \\
&\quad \times [e^{i[2\xi(s,s') - \alpha(s') - \alpha(s)]} + e^{2i[\xi(s,s') - \alpha(s')]}] \frac{H_1^{(1)}[k\rho(s,s')]}{\rho(s,s')} \\
&\quad + k\frac{[\mathcal{K}^{-1} - \mathcal{K}]}{2}.
\end{aligned} \tag{B9}$$

Using the BIEs Eq. (12) and Eq. (13) it can be shown that the second integral equals

$$\begin{aligned}
&\frac{ik}{4}\oint_{\partial\Omega} ds \psi_1^*(s)\left\{[e^{i[\alpha(s') - \alpha(s)]} + 1] k H_0^{(1)}[k\rho(s,s')] \right. \\
&\quad \left. - [\mathcal{K} e^{i[\alpha(s') - \alpha(s)]} + \mathcal{K}^{-1}] e^{i[\xi(s,s') - \alpha(s')]} k H_1^{(1)}[k\rho(s,s')]\right\} \\
&= -k\frac{[\mathcal{K}^{-1} - \mathcal{K}]}{2} \\
&\quad - 2\frac{ik}{4}\oint_{\partial\Omega} ds \psi_1^*(s) \mathcal{K}^{-1} k H_1^{(1)}[k\rho(s,s')] \cos[\xi(s,s') \\
&\quad - \alpha(s')].
\end{aligned}$$

With $\cos\theta_\beta \mathcal{K} = 1 - \sin\theta_\beta$, $\cos\theta_\beta \mathcal{K}^{-1} = 1 + \sin\theta_\beta$, and $\frac{\mathcal{K}^{-1} - \mathcal{K}}{2} = \beta = \frac{\sin\theta_\beta}{\cos\theta_\beta}$ Eq. (26) is recovered. The same result is obtained when applying the normal derivatives to Eqs. (12) and (13).

In the semiclassical limit the last term in Eq. (26) approaches

$$\frac{H_1^{(1)}[k\rho(s,s')]}{k\rho(s,s')} = \frac{H_0^{(1)}[k\rho(s,s')] + H_2^{(1)}[k\rho(s,s')]}{2} \tag{B10}$$

$$\xrightarrow{k\to\infty} -i\sqrt{\frac{2}{\pi k\rho}} e^{ik\rho - \frac{i}{4}\pi}\frac{2}{k\rho}, \tag{B11}$$

which is by a factor $\frac{1}{k\rho}$ smaller than $H_0^{(1)}[k\rho(s,s')]$ in Eq. (34) and $H_1^{(1)}[k\rho(s,s')]$ in Eq. (35). Since we exclude billiards with corners, that is, $\rho(s,s')$ is nonzero along POs of nonzero lengths, we may disregard this term in the derivation of the trace formula.

The $\cos\theta_\beta$ term in the curly bracket of the product $\tilde{\mathcal{P}}_p^*$ in Eq. (43) does not factorize into the denominator of Eq. (38) and a term, which is nonsingular for $\chi_r = \pi/2$ and thus needs to be handled cautiously when evaulating the trace formula. Using the relation

$$\begin{aligned}
&\prod_{r=1}^{p}\left[\cos\left(\frac{\chi_r + \chi_{r+1}}{2}\right) + \sin\left(\frac{\chi_r - \chi_{r+1}}{2}\right)\right] \\
&\quad = \prod_{r=1}^{p}\left[\cos\left(\frac{\chi_r}{2}\right) + \sin\left(\frac{\chi_r}{2}\right)\right]\left[\cos\left(\frac{\chi_{r+1}}{2}\right)\right. \\
&\quad \left. - \sin\left(\frac{\chi_{r+1}}{2}\right)\right] \\
&\quad = \prod_{r=1}^{p}\cos\chi_r \\
&\quad = \prod_{r=1}^{p}\left\{2\cos\left(\frac{\chi_r}{2} - \frac{\pi}{4}\right)\cos\left(\frac{\chi_{r+1}}{2} + \frac{\pi}{4}\right)\right\}
\end{aligned} \tag{B12}$$

it can be brought to the form

$$\begin{aligned}
&\prod_{r=1}^{p}\left[-\frac{\cos\theta_\beta}{\cos\chi_r}\right] \\
&\quad \times \left[\cos\left(\frac{\chi_r + \chi_{r+1}}{2}\right) - i\sin\theta_\beta \sin\left(\frac{\chi_r + \chi_{r+1}}{2}\right)\right. \\
&\quad \left. + \cos\theta_\beta \sin\left(\frac{\chi_r - \chi_{r+1}}{2}\right)\right] \\
&= \prod_{r=1}^{p}[-\cos\theta_\beta] \\
&\quad \times \left\{\cos\theta_\beta + \frac{1 - \cos\theta_\beta}{2}\left[1 - \tan\left(\frac{\chi_r}{2} - \frac{\pi}{4}\right)\right.\right.
\end{aligned}$$

$$\times \tan\left(\frac{\chi_{r+1}}{2}+\frac{\pi}{4}\right)\Big] - i\frac{\sin\theta_\beta}{2}\Big[\tan\left(\frac{\chi_r}{2}-\frac{\pi}{4}\right)+\tan\left(\frac{\chi_{r+1}}{2}+\frac{\pi}{4}\right)\Big]\Big\}. \tag{B13}$$

The reflection angles χ_r, $r = 1, \ldots, p+1$ take values in $\chi_r \in (-\frac{\pi}{2}, \frac{\pi}{2})$. Thus the second and third terms in the curly brackets become large for $\chi_r = \frac{\pi}{2}$ and for $\chi_{r+1} = -\frac{\pi}{2}$. Note, that the prefactors of the terms become small in the ultrarelativistic limit $\theta_\beta \to 0$ and the whole term vanishes in the nonrelativistic limit $\theta_\beta \to \frac{\pi}{2}$.

[1] Y. G. Sinai, Russ. Math. Surv. **25**, 137 (1990).
[2] L. A. Bunimovich, Commun. Math. Phys. **65**, 295 (1979).
[3] M. V. Berry, Eur. J. Phys. **2**, 91 (1981).
[4] *Chaos and Quantum Physics*, edited by M. Giannoni, A. Voros, and J. Zinn-Justin (Elsevier, Amsterdam, 1989).
[5] H.-J. Stöckmann and J. Stein, Phys. Rev. Lett. **64**, 2215 (1990).
[6] A. Richter, in *Emerging Applications of Number Theory, The IMA Volumes in Mathematics and Its Applications*, edited by D. A. Hejhal, J. Friedman, M. C. Gutzwiller, and A. M. Odlyzko (Springer, New York, 1999), Vol. 109, p. 479.
[7] F. Haake, *Quantum Signatures of Chaos* (Springer-Verlag, Heidelberg, 2001).
[8] S. Sridhar, Phys. Rev. Lett. **67**, 785 (1991).
[9] H.-D. Gräf, H. L. Harney, H. Lengeler, C. H. Lewenkopf, C. Rangacharyulu, A. Richter, P. Schardt, and H. A. Weidenmüller, Phys. Rev. Lett. **69**, 1296 (1992).
[10] J. Stein and H.-J. Stöckmann, Phys. Rev. Lett. **68**, 2867 (1992).
[11] P. So, S. M. Anlage, E. Ott, and R. N. Oerter, Phys. Rev. Lett. **74**, 2662 (1995).
[12] S. Deus, P. M. Koch, and L. Sirko, Phys. Rev. E **52**, 1146 (1995).
[13] B. Dietz and A. Richter, Chaos **25**, 097601 (2015).
[14] M. V. Berry and M. Tabor, J. Phys. A **10**, 371 (1977).
[15] M. Berry, in *Structural Stability in Physics*, edited by W. Güttinger and H. Eikemeier, Springer Series of Synergetics (Springer-Verlag, Berlin, 1979).
[16] G. Casati, F. Valz-Gris, and I. Guarnieri, Lett. Nuovo Cimento **28**, 279 (1980).
[17] O. Bohigas, M. J. Giannoni, and C. Schmit, Phys. Rev. Lett. **52**, 1 (1984).
[18] M. V. Berry, J. Phys. A **10**, 2083 (1977).
[19] M. C. Gutzwiller, J. Math. Phys. **12**, 343 (1971).
[20] M. C. Gutzwiller, *Chaos in Classical and Quantum Mechanics* (Springer, Berlin, 1990).
[21] S. Heusler, S. Müller, A. Altland, P. Braun, and F. Haake, Phys. Rev. Lett. **98**, 044103 (2007).
[22] F. Leyvraz, C. Schmit, and T. H. Seligman, J. Phys. A **29**, L575 (1996).
[23] C. Dembowski, H.-D. Gräf, A. Heine, H. Rehfeld, A. Richter, and C. Schmit, Phys. Rev. E **62**, R4516 (2000).
[24] C. Dembowski, B. Dietz, H.-D. Gräf, H. L. Harney, A. Heine, W. D. Heiss, and A. Richter, Phys. Rev. Lett. **90**, 034101 (2003).
[25] O. Knill, Elem. Math. **53**, 89 (1998).
[26] B. Gutkin, J. Phys. A **40**, F761 (2007).
[27] G. Veble, T. Prosen, and M. Robnik, New J. Phys. **9**, 15 (2007).
[28] B. Dietz, T. Guhr, B. Gutkin, M. Miski-Oglu, and A. Richter, Phys. Rev. E **90**, 022903 (2014).
[29] S. C. Creagh and R. G. Littlejohn, Phys. Rev. A **44**, 836 (1991).
[30] T. H. Seligman and H. A. Weidenmüller, J. Phys. A **27**, 7915 (1994).
[31] C. H. Joyner, S. Müller, and M. Sieber, J. Phys. A **45**, 205102 (2012).
[32] M. V. Berry and R. J. Mondragon, Proc. R. Soc. Lond. A **412**, 53 (1987).
[33] P. G. Silvestrov and K. B. Efetov, Phys. Rev. Lett. **98**, 016802 (2007).
[34] L. A. Ponomarenko, F. Schedin, M. I. Katsnelson, R. Yang, E. W. Hill, K. S. Novoselov, and A. K. Geim, Science **320**, 5874 (2008).
[35] F. Libisch, C. Stampfer, and J. Burgdörfer, Phys. Rev. B **79**, 115423 (2009).
[36] J. Wurm, A. Rycerz, İ. Adagideli, M. Wimmer, K. Richter, and H. U. Baranger, Phys. Rev. Lett. **102**, 056806 (2009).
[37] L. Huang, Y.-C. Lai, D. K. Ferry, S. M. Goodnick, and R. Akis, Phys. Rev. Lett. **103**, 054101 (2009).
[38] L. Huang, Y.-C. Lai, and C. Grebogi, Phys. Rev. E **81**, 055203(R) (2010).
[39] J. Wurm, K. Richter, and İ. Adagideli, Phys. Rev. B **84**, 075468 (2011).
[40] A. Rycerz, Phys. Rev. B **85**, 245424 (2012).
[41] A. Rycerz, Phys. Rev. B **87**, 195431 (2013).
[42] M. Polini, F. Guinea, M. Lewenstein, H. C. Manoharan, and V. Pellegrini, Nat. Nanotechnol. **8**, 625 (2013).
[43] B. Dietz, T. Klaus, M. Miski-Oglu, and A. Richter, Phys. Rev. B **91**, 035411 (2015).
[44] B. Dietz, T. Klaus, M. Miski-Oglu, A. Richter, M. Wunderle, and C. Bouazza, Phys. Rev. Lett. **116**, 023901 (2016).
[45] K. S. Novoselov, A. K. Geim, S. V. Morozov, D. Jiang, Y. Zhang, S. V. Dubonos, I. V. Grigorieva, and A. A. Firsov, Science **306**, 666 (2004).
[46] C. W. J. Beenakker, Rev. Mod. Phys. **80**, 1337 (2008).
[47] A. H. Castro Neto, F. Guinea, N. M. R. Peres, K. S. Novoselov, and A. K. Geim, Rev. Mod. Phys. **81**, 109 (2009).
[48] Y.-C. Lai, H.-Y. Xu, L. Huang, and C. Grebogi, Chaos **28**, 052101 (2018).
[49] L. Huang, H.-Y. Xu, C. Grebogi, and Y.-C. Lai, Phys. Rep. **753**, 1 (2018).
[50] B. Dietz and A. Richter, Phys. Scr. **94**, 014002 (2019).
[51] J. Bolte and S. Keppeler, Ann. Phys. **274**, 125 (1999).
[52] S. Keppeler, Ann. Phys. **304**, 40 (2003).
[53] P. Carmier and D. Ullmo, Phys. Rev. B **77**, 245413 (2008).
[54] B. Dietz, Acta Phys. Pol. A **136**, 770 (2019).
[55] T. Harayama and A. Shudo, Phys. Lett. A **165**, 417 (1992).
[56] M. Sieber, J. Phys. A **30**, 4563 (1997).
[57] M. Sieber, Nonlinearity **11**, 1607 (1998).
[58] M. Berry, Proc. R. Soc. Lond. A **430**, 405 (1990).
[59] M. Sieber and F. Steiner, Phys. Rev. Lett. **67**, 1941 (1991).
[60] E. B. Bogomolny, Nonlinearity **5**, 805 (1992).

[61] M.-Y. Song, Z.-Y. Li, H.-Y. Xu, L. Huang, and Y.-C. Lai, Phys. Rev. Res. **1**, 033008 (2019).
[62] M. Sieber, U. Smilansky, S. C. Creagh, and R. G. Littlejohn, J. Phys. A **26**, 6217 (1993).
[63] S. M. Reimann, M. Brack, A. G. Magner, J. Blaschke, and M. V. N. Murthy, Phys. Rev. A **53**, 39 (1996).
[64] G. Baym, *Lectures on Quantum Mechanics* (CRC Press, Boca Raton, FL, 2018).
[65] M. Sieber, H. Primack, U. Smilansky, I. Ussishkin, and H. Schanz, J. Phys. A **28**, 5041 (1995).
[66] M. V. Berry and M. R. Dennis, J. Phys. A **41**, 135203 (2008).
[67] P. Yu, B. Dietz, and L. Huang, New J. Phys. **21**, 073039 (2019).
[68] A. Bäcker, *Numerical Aspects of Eigenvalue and Eigenfunction Computations for Chaotic Quantum Systems* (Springer, Berlin, 2003), pp. 91–144.
[69] P. Yu, B. Dietz, H.-Y. Xu, L. Ying, L. Huang, and Y.-C. Lai, Phys. Rev. E **101**, 032215 (2020).
[70] H.-J. Stöckmann, *Quantum Chaos: An Introduction* (Cambridge University Press, Cambridge, 2000).
[71] R. Balian and B. Duplantier, Ann. Phys. (NY) **104**, 300 (1977).
[72] C. Dembowski, B. Dietz, H.-D. Gräf, A. Heine, T. Papenbrock, A. Richter, and C. Richter, Phys. Rev. Lett. **89**, 064101 (2002).
[73] B. Dietz, B. Mößner, T. Papenbrock, U. Reif, and A. Richter, Phys. Rev. E **77**, 046221 (2008).
[74] J. P. Keating and M. Sieber, Proc. R. Soc. Lond. A **447**, 413 (1994).
[75] J. P. Keating and S. Müller, Proc. R. Soc. Lond. A **463**, 3241 (2007).
[76] B. Gutkin, Proc. Am. Math. Soc. **137**, 2795 (2009).
[77] L. Bunimovich and G. Magno, Commun. Math. Phys. **288**, 699 (2009).
[78] S. Keshavamurthy and P. Schlagheck, *Dynamical Tunneling-Theory and Experiment* (CRC Press, Boca Raton, FL, 2011).
[79] R. E. Kleinman and G. F. Roach, SIAM Rev. **16**, 214 (1974).